PCCP

Cite this: *Phys. Chem. Chem. Phys.*, 2012, **14**, 11268–11272

www.rsc.org/pccp

COMMUNICATION

Differential capacitance of liquid/liquid interfaces of finite thicknesses: a finite element study†

Dmitry Momotenko,[a] Carlos M. Pereira[b] and Hubert H. Girault*[a]

Received 4th May 2012, Accepted 25th June 2012
DOI: 10.1039/c2cp41437f

Finite element simulations were used to investigate the effect of a smooth variation of permittivity across a polarized liquid/liquid interface on the differential capacitance. The results show that a relative permittivity profile can account for the variation of ion solvation in the interfacial region, and therefore upon the diffuse double layer itself. The width and the symmetry of this profile across the interface are shown to be crucial parameters for interfacial distributions and fitting of capacitance data has been used to estimate the width of the interfacial region.

Physico-chemical properties of liquid/liquid interfaces are of interest particularly due to their extensive industrial applications, such as liquid–liquid extraction and liquid chromatography,[1] nanochemical reactions in micellar systems,[2] catalysis,[3,4] drug delivery in pharmacology[5] and artificial photosynthetic systems.[6,7] Understanding fundamental processes occurring at the interface between two immiscible electrolyte solutions (ITIES) such as ion and electron transfer, electrical potential and ion distributions, adsorption, solvation, *etc.* is therefore of prime importance. In most cases, the interfaces are treated without taking into account the thickness of the interfacial region, *i.e.* the interphase exhibiting transitional properties between the two bulk phases. The structure of this intermediate interfacial layer is generally unknown since it is difficult to probe its microscopic properties at the molecular level. The available set of experimental techniques (X-ray methods,[8,9] surface second harmonic generation[10] and neutron scattering)[9,11] is somehow limited as most of the techniques provide macroscopic quantities that are difficult to interpret at the molecular level. Instead, one can account for interfacial parameters with the use of molecular dynamics[12–14] and Monte-Carlo[15,16] simulations.

The phenomenological description of ionic and potential distributions at ITIES is usually given by solving the Poisson–Boltzmann equation, where the energy of point charges is assumed to follow a Boltzmann relationship based only on electrostatic interactions. Therefore, the interface between two immiscible liquids could be considered as a non-permeable infinitely thin layer separating two back-to-back Gouy–Chapman layers propagating towards bulk phases. However, the reported experimental data usually deviate from predictions of the simple Gouy–Chapman theory,[8,17–20] most likely, due to the fact that structural properties of the electrolyte solution, such as finite ion size, ion–ion interactions, are ignored within such a simplified approach. Solving the Poisson equation by taking into account ion solvation terms along with purely electrostatic energy factors was used in a simplified analytical model developed by Kharkats and Ulstrup.[21] More recently, Schlossman *et al.* calculated the potential mean force of a single ion based on molecular dynamics calculations to reconstruct the total ion distribution.[8] The interface in these approaches is treated as dielectric medium with constant relative permittivity ε_r[8] or by assuming a sharp discontinuity of dielectric properties at the interface, that is disregarding the effect of the interphase width.[21]

In this communication, we present a simple finite element approach for the simulations of differential capacitance of the water/1,2-dichloroethane (DCE) interface taking into account an interfacial width defined through the distribution of the relative permittivity ε_r. The gist of this approach is to encode within a single macroscopic quantity, namely the relative permittivity, not only all the variations of solvent composition within the interphase but also all the long-range dipolar interactions of a single ion as it approaches the interface, *i.e.* the overall variation of the Gibbs energy of solvation. The comparison with experimental data shows the advantage of this methodology *versus* the classical Gouy–Chapman approach in estimating electrochemical properties at electrified liquid/liquid interfaces. Finite element modeling was performed using the commercially available package COMSOL Multiphysics (version 3.5a) operating under Linux Ubuntu 8.04 environment installed on a Mac Pro with four 2.66 GHz central processing units and 9.8 Gb of RAM. One-dimensional computational domain of 1 μm in length was divided into two equal subdomains representing aqueous and organic electrolyte solutions, centered at the origin of the x coordinate axis denoting the liquid/liquid boundary, where the ions cannot permeate. Both the Poisson equation (eqn (1)), describing electrical potential ϕ

$$\nabla^2\phi = -\frac{F}{\varepsilon_r\varepsilon_0}\sum_i z_i c_i \qquad (1)$$

[a] *Laboratoire d'Electrochimie Physique et Analytique, Ecole Polytechnique Fédérale de Lausanne, Station 6, CH-1015 Lausanne, Switzerland. E-mail: hubert.girault@epfl.ch; Fax: +41-21-693 3667; Tel: +41-21-693 3145*
[b] *CIQ-UP L4, Faculdade de Ciências, Universidade do Porto, Rua do Campo Alegre 687, 4169-007 Porto, Portugal*

† Electronic supplementary information (ESI) available: Details of the simulation procedure, model validation, equation system formulation taking into account ion solvation effects. See DOI: 10.1039/c2cp41437f

and the Nernst–Planck equation (eqn (2)) for the computation of ionic fluxes J_i

$$J_i = -D_i\nabla c_i - \frac{z_i F}{RT} D_i c_i \nabla\phi + uc_i \qquad (2)$$

were solved in each domain for 1 : 1 electrolyte. Here D_i, c_i, z_i, F, R, T, ϕ, u denote the diffusion coefficient, concentration, charge number of species i, Faraday constant, gas constant, temperature, electric potential and fluid velocity, respectively, while ε_0 represents the vacuum permittivity.

Numerical resolution of the coupled Nernst–Planck–Poisson equation system was then computed using 2626 mesh elements (mesh size at the interface point was refined down to 10^{-14} m) corresponding to 15 761 degrees of freedom. The model was validated by comparing numerical results with analytical calculations within the framework of the Gouy–Chapman theory giving the relative error value of simulated results of less than 0.3% (see more details in ESI†).

The microscopic consideration of the liquid/liquid interphase requires treating the physico-chemical parameters of the medium to change smoothly within a thin interfacial region. This could be performed with the use of molecular dynamic simulations for particular phases brought into contact[22–24] or by considering the interfacial region as a mixed solvent layer followed by estimation of relative permittivity as the function of molar fraction of polar or non-polar co-solvent.[25] Herein, we treat the continuity of dielectric properties of the liquid medium by using a sigmoid-like approximation of relative permittivity (eqn (3))

$$\varepsilon_r = \varepsilon_{aq} + \frac{f(\varepsilon_{org} - \varepsilon_{aq})}{f + e^{x/a}} \qquad (3)$$

As can be seen from Fig. 1, ε_r distribution is represented as a continuous and smooth change of dielectric properties between bulk phases defined as ε_{aq} and ε_{org} for aqueous and organic electrolyte solutions, respectively. The symmetry factor f defines the degree of penetration of the interphase into each bulk solution, *e.g.* shifting ε_r distribution towards the organic ($f < 1$) or aqueous part ($f > 1$) with respect to the $x = 0$ plane. In the symmetrical case ($f = 1$) equation (eqn (3)) reads

$$\varepsilon_r = \varepsilon_{aq} + \frac{\varepsilon_{org} - \varepsilon_{aq}}{1 + e^{x/a}} = \varepsilon_s + \left(\frac{\varepsilon_{aq} - \varepsilon_{org}}{2}\right)\tanh\left[\frac{x}{2a}\right] \qquad (4)$$

where the value of dielectric constant at the interface ($x = 0$) is given by

$$\varepsilon_s = \frac{\varepsilon_{org} + \varepsilon_{aq}}{2} \qquad (5)$$

Therefore, the interfacial width $\lambda^{S,\alpha}$ in each phase α could be defined as

$$\lambda^{S,\alpha} = 2a \qquad (6)$$

giving the total thickness of the interphase, $\lambda^S = 2\lambda^{S,\alpha} = 4a$. In a first approximation one can assume that the interfacial thickness λ^S is governed mainly by the a parameter taking into account that the f factor only contributes for symmetry of dielectric constant ε_r across the impermeable liquid/liquid boundary. Hence, the description of the relative dielectric permittivity profile is governed by reciprocal width a of the interphase and its relative position with respect to the interfacial plane, that is only two parameters control smooth variation of solvent properties.

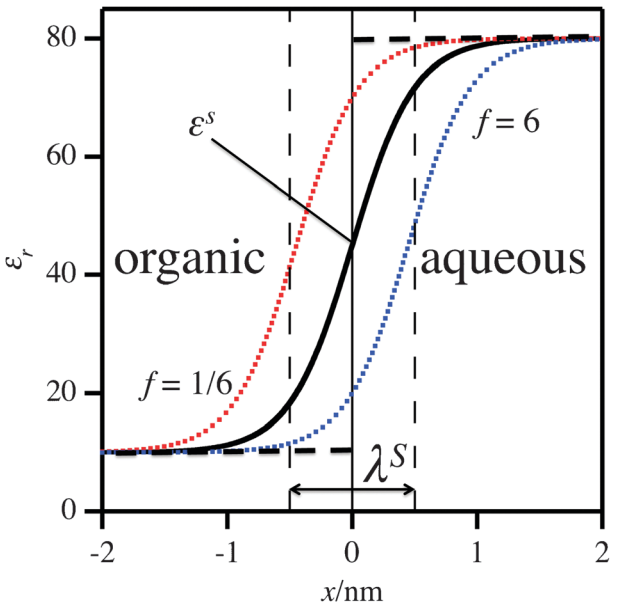

Fig. 1 Distribution of relative permittivity ε_r (according to eqn (3)) calculated for interfacial width λ^S of 1 nm in the symmetric case (solid line, $f = 1$) and for interphase penetrating organic (dotted line, $f = 1/6$) or aqueous (blue line, $f = 6$) bulk electrolytes compared to the classical Gouy–Chapman step function (dashed thick lines). Thin dashed lines denote the location of an interphase. The impermeable liquid–liquid boundary, *i.e.* the interface is located at $x = 0$.

Fig. 2 demonstrates the influence of interfacial region width λ^S on the distribution of electrical potential near the interface. As can be seen, the effect of discontinuity of dielectric properties within the Gouy–Chapman theory results in an unrealistic non-linear potential change across the liquid/liquid boundary. In contrast, the electrical potential profile smoothes when taking into account interfacial width λ^S and shows symmetrical behavior at relatively large λ^S values. Similarly, values of interfacial electrical potential ϕ^S (Fig. 2b) swap from sigmoid-like shape for infinitely thin interface into a linear relation with the potential differences applied across bulk phases. In other words, ϕ^S tends to the medial values with the increase of interfacial thickness λ^S, *i.e.* intermediate with respect to potential difference $\Delta\phi$ applied. These results indicate a more realistic approach through a relative permittivity distribution. Classical Gouy–Chapman theory assuming discontinuity of ε_r at the interface does not consider the rearrangement of ion solvation at the interface leading to unrealistically sharp variations of electrochemical properties and ion distributions at the liquid/liquid boundary. In contrast, the present approach takes into account the electrostatic part of these interactions taking place within the interphase in a global manner with a single parameter, namely ε_r.

Typically, being exceptionally important parameters for interfacial processes (*e.g.* ion and electron transfer, adsorption and solvent extraction), microscopic interfacial potential and ion distributions at ITIES are experimentally inaccessible. Instead, one has to address macroscopic quantities related to

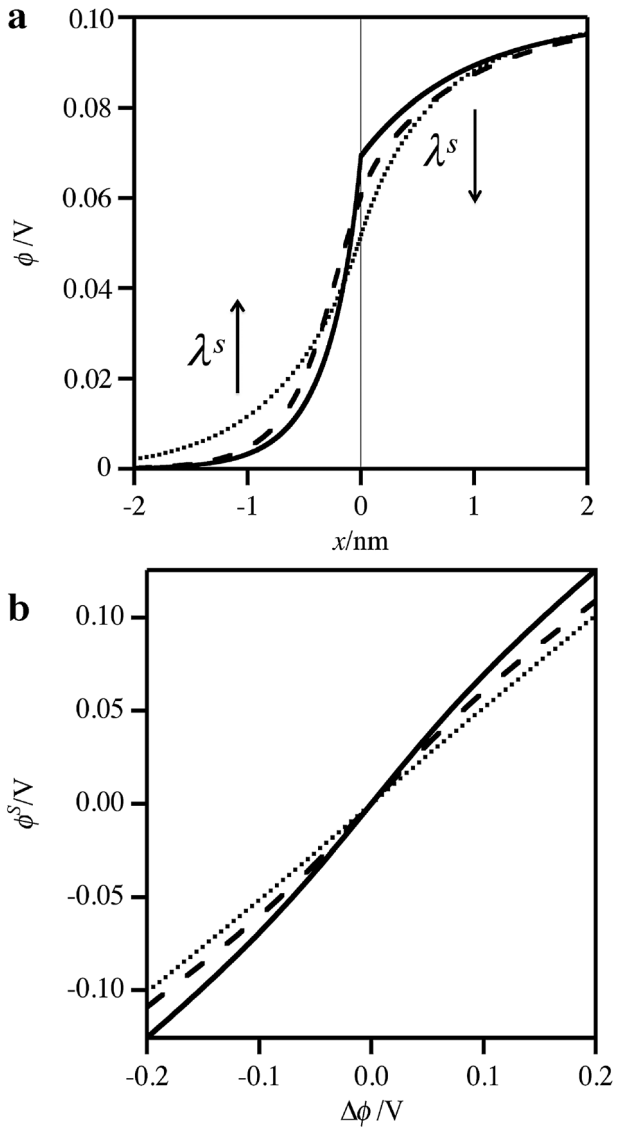

Fig. 2 (a) Interfacial distributions of electric potential ϕ calculated at different interfacial widths λ^S and (b) simulated interfacial electrical potential ϕ^S (*i.e.* the value calculated at $x = 0$) over the applied Galvani potential difference $\Delta\phi$ for λ^S equal to 0 (Gouy–Chapman case), 0.4 nm and 5.33 nm for solid, dashed and dotted lines, respectively. Arrows in the graph indicate increase of interphase thickness λ^S.

interfacial structure like differential capacitance C_d determined as the ability to store charge σ in response to a perturbation potential

$$C_d = \pm\frac{\partial\sigma}{\partial(\phi^s - \phi^\infty)} \tag{7}$$

where $(\phi^S - \phi^\infty)$ determines the drop in the potential of the electrolyte. Herein, it is convenient to represent surface charge as

$$\sigma = -\varepsilon_r\varepsilon_0\left(\frac{\partial\phi(x)}{\partial x}\right)_{x=0} = -\varepsilon_r\varepsilon_0\left(\frac{\partial\phi^S}{\partial x}\right) \tag{8}$$

and calculate the overall capacitance considering capacitive contributions C_d^{aq} and C_d^{org} from aqueous and DCE phases, respectively, as capacitors in series

$$C_d = \frac{C_d^{aq}C_d^{org}}{C_d^{aq} + C_d^{org}} \tag{9}$$

Fig. 3a shows the influence of interfacial layer thickness on the value of total differential capacitance of the ITIES at constant electrolyte concentrations. As can be seen, the deviation from classical Gouy–Chapman behaviour increases with the expansion of the interfacial region resulting in an overall increase of differential capacitance. This effect is mostly pronounced at

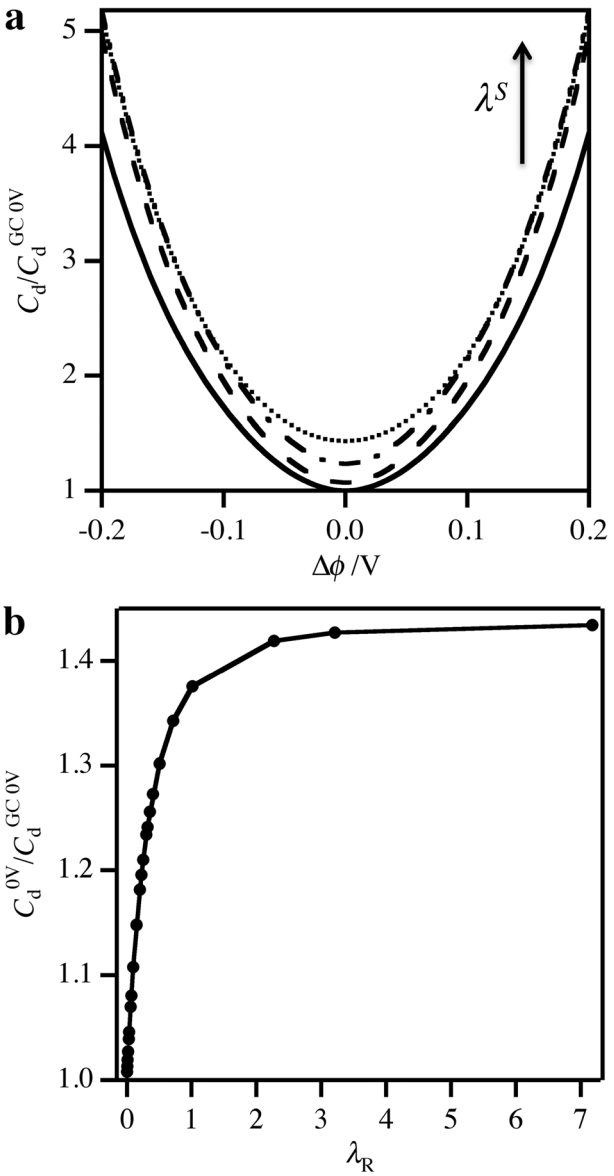

Fig. 3 (a) Simulated differential capacitance curves (relative to the differential capacitance $C_d^{GC\ 0V}$ at potential of zero charge (pzc) calculated within frameworks of Gouy–Chapman theory) at the water/DCE interface containing 1 : 1 electrolyte at a bulk concentration of 100 mM. Solid, dashed, dash-dotted and dotted curves correspond to various interfacial widths λ^S equal to 0 (Gouy–Chapman case), 0.08 nm, 0.4 nm and 5.33 nm. The arrow in the graph indicates an increase of interphase thickness λ^S. (b) Relative differential capacitance at pzc $C_d^{0V}/C_d^{GC\ 0V}$ as the function of interfacial thickness compared to the size of the diffuse layer.

the potential of zero charge (pzc) where the gradual increase of differential capacitance follows the growth of interfacial region size λ^S, while C_d curves coincide at higher voltage perturbations, most likely due to the compression of diffuse layers. Instead of operating with an interfacial width λ^S, it is more convenient to use a dimensionless quantity λ^R which is taken as the interphase thickness normalized by the Debye–Hückel length λ_α^D calculated for both phases having a relative permittivity ε_r^α and containing electrolyte at bulk concentration c_0

$$\lambda^R = \frac{\lambda^S}{\lambda_{aq}^D + \lambda_{org}^D} \tag{10}$$

$$\lambda_\alpha^D = \frac{\varepsilon_r^\alpha \varepsilon_0 RT}{2F^2 c_0} \tag{11}$$

Fig. 3b summarizes the data of relative capacitance at pzc (normalized to that predicted from Gouy–Chapman relation) computed at various interfacial thicknesses and electrolyte concentrations. In very dilute solutions the size of the liquid/liquid interphase could be assumed to be negligibly small compared to the characteristic Debye length and the capacitive behavior of the ITIES does not significantly deviate from that predicted by Gouy–Chapman's model. At higher electrolyte concentrations, however, the discontinuity of the relative permittivity cannot be anymore suspected and the effect of the interphase plays an important role in ion and potential distributions causing noticeable discrepancy with Gouy–Chapman behavior. Therefore, the interfacial width compared to the diffuse layer size could be regarded as one of the key parameters predicting capacitive behavior at ITIES regardless of λ^S and electrolyte concentrations. Compared to reports of Daikhin *et al.*[26,27] considering smearing of dielectric properties across the ITIES in a "mixed layer" within a perturbation approach the current model is advantageous as no limitations to electrolyte concentration and/or thickness of the interfacial layer are introduced into the calculations.

In order to demonstrate the importance of interfacial contribution to the electrochemical behavior of electrified ITIES, it is convenient to proceed with the comparison between simulated differential capacitance and experimental data (from Pereira *et al.*[17]) shown in Fig. 4. Typically, predictions of classical Gouy–Chapman theory underestimate the measured values of capacitance behavior, however, this could be overcome by taking into account the finite size of the interphase. The size of this interfacial zone where the physical properties (such as density and interfacial tension, for instance) of the medium take transitional values depends on polarity (*i.e.* dipole moment) of both liquid phases and therefore varies with the different type of solvents used.[28] The water/DCE interfacial thickness was estimated to be in the order of nanometers.[29] In this study, we examined capacitive properties of water/DCE interfaces of thickness up to 5.33 nm, however, the obtained results do not match the experimental values although an improvement compared to Gouy–Chapman values is observed. Most likely, it indicates the asymmetry of dielectric properties with respect to the impermeable boundary located at the interface (at $x = 0$), *i.e.* the penetration of interphase towards into one of the bulk phases. This hypothesis is not an unrealistic scenario as

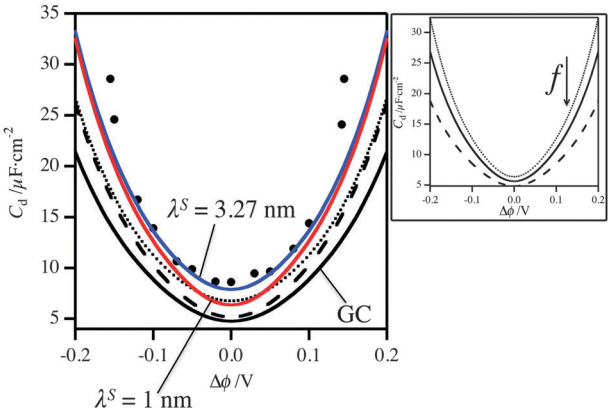

Fig. 4 Differential capacitance C_d for the systems: Ag|AgCl|KCl 10 mM, aq‖tetrabutylammonium tetraphenylborate 10 mM, DCE|tetrabutylammonium chloride 10 mM, aq|AgCl|Ag. Dots represent experimental values, simulated data are represented as curves: black solid, dashed and dotted lines denote the variation of thicknesses λ^S, *i.e.* 0 (from Gouy–Chapman theory), 0.4 nm and 5.33 nm, respectively, while solid C_d curves for λ^S of 1 nm and 3.27 nm show the calculated data for interphase penetrating the organic phase ($f = 1/6$). The inset on the right shows the influence of the f factor (1, 6 and 1/6 for solid, dashed and dotted lines, respectively) on the capacitance of the system considering an interfacial width of 1 nm.

the interfacial structure is *a priori* unknown and asymmetric behavior (*e.g.* in solvation energy) could take place at ITIES.[21] Our results indicate that even a relatively small penetration of interphase ε_r with respect to the impermeable boundary results in a remarkable change of capacitive behavior. The inset of Fig. 4 shows the corresponding change in differential capacitance with variation of the f parameter that defines the degree of ε_r asymmetry. As demonstrated, the penetration of the interfacial region into DCE solution results in an overall increase of C_d. Numerical modeling performed with consideration of the f parameter resulted in a good approximation of experimental data with a 1–3 nm thick interphase, suggesting the validity of this approach.

The versatility of the proposed strategy allows also incorporation of ion–solvent interactions into a numerical model *via*, for example, Born approximation. In such a case the energy of ion solvation is reciprocal to relative permittivity ε_r and ionic radius r_{ion}, *i.e.*

$$\Delta G_{IS} = -\frac{z_i^2 e^2 N_a}{8\pi\varepsilon_0 r_{ion}}\left(1 - \frac{1}{\varepsilon_r}\right) \tag{12}$$

where e and N_a denote elementary charge and Avogadro's constant, respectively. Therefore this relation could be incorporated as a standard chemical potential term μ_i^0 into the flux equation

$$\begin{aligned} J_i &= -\frac{D_i}{RT} c_i \nabla \mu_i \\ &= \left[-D_i \nabla c_i - \frac{z_i F}{RT} D_i c_i \nabla \phi\right] - \frac{D_i}{RT} c_i \nabla \mu_i^0 \end{aligned} \tag{13}$$

However, the contribution of the ion–solvent interaction to ion and potential distributions is very weak (see SI-3 in the ESI†).

In summary, we have investigated the influence of interfacial width on the electrochemical behavior of the ITIES using

simple numerical methodology. The sigmoid-like relative permittivity distribution propagating across the liquid/liquid boundary defined the structure of an interphase layer affecting ion and potential distributions as well as the capacitive behavior of the ITIES. According to the numerical results the key parameter defining electrochemical properties of electrified interfaces is the thickness of this interfacial region compared to the size of the diffuse layer. In contrast to the classical Gouy–Chapman approach disregarding the effect of the interfacial layer our modeling suggested more realistic behavior of the electrolyte at charged ITIES predicting smaller deviation of simulated differential capacitance from experimentally measured values. Compared to other methods, such as molecular dynamics simulations, this approach has certain advantages, as it incorporates numerically effortless one-dimensional finite-element modeling. As demonstrated, the framework of the present numerical approach allows us to overcome the idealistic prerequisites of Gouy–Chapman theory by introducing solvation effects and treating the finite ion size within a partial differential equation system. The versatility of the numerical model could also be extended with the effect of ion–ion interactions through Debye–Hückel theory and/or by taking into account changes of relative permittivity with local ionic strength of electrolyte solutions.

One of us, C.M.P, is grateful to the EPFL for a visiting professorship.

Notes and references

1 A. G. Volkov, *Liquid interfaces in chemical, biological, and pharmaceutical applications*, Marcel Dekker, New York, 2001.
2 V. Uskokovic and M. Drofenik, *Adv. Colloid Interface Sci.*, 2007, **133**, 23–34.
3 A. Trojanek, J. Langmaier, B. Su, H. H. Girault and Z. Samec, *Electrochem. Commun.*, 2009, **11**, 1940–1943.
4 J. J. Nieminen, I. Hatay, P. Y. Ge, M. A. Mendez, L. Murtomaki and H. H. Girault, *Chem. Commun.*, 2011, **47**, 5548–5550.
5 K. K. Jain, *Drug delivery systems*, Humana, Totowa, NJ, 2008.
6 R. Lahtinen, D. J. Fermin, K. Kontturi and H. H. Girault, *J. Electroanal. Chem.*, 2000, **483**, 81–87.
7 D. Schaming, I. Hatay, F. Cortez, A. Olaya, M. A. Mendez, P. Y. Ge, H. Q. Deng, P. Voyame, Z. Nazemi and H. Girault, *Chimia*, 2011, **65**, 356–359.
8 G. M. Luo, S. Malkova, J. Yoon, D. G. Schultz, B. H. Lin, M. Meron, I. Benjamin, P. Vanysek and M. L. Schlossman, *Science*, 2006, **311**, 216–218.
9 M. L. Schlossman, *Curr. Opin. Colloid Interface Sci.*, 2002, **7**, 235–243.
10 H. Nagatani, A. Piron, P. F. Brevet, D. J. Fermin and H. H. Girault, *Langmuir*, 2002, **18**, 6647–6652.
11 J. Bowers, A. Zarbakhsh, J. R. P. Webster, L. R. Hutchings and R. W. Richards, *Langmuir*, 2001, **17**, 140–145.
12 D. Michael and I. Benjamin, *J. Chem. Phys.*, 2001, **114**, 2817–2824.
13 A. R. Vanbuuren, S. J. Marrink and H. J. C. Berendsen, *J. Phys. Chem.*, 1993, **97**, 9206–9212.
14 J. P. Nicolas and N. R. de Souza, *J. Chem. Phys.*, 2004, **120**, 2464–2469.
15 P. Linse, *J. Chem. Phys.*, 1987, **86**, 4177–4187.
16 S. Frank and W. Schmickler, *J. Electroanal. Chem.*, 2004, **564**, 239–243.
17 C. M. Pereira, A. Martins, M. Rocha, C. J. Silva and F. Silva, *J. Chem. Soc., Faraday Trans.*, 1994, **90**, 143–148.
18 C. Yufei, V. J. Cunnane, D. J. Schiffrin, L. Mutomaki and K. Kontturi, *J. Chem. Soc., Faraday Trans.*, 1991, **87**, 107–114.
19 N. Laanait, J. Yoon, B. Hou, P. Vanysek, M. Meron, B. Lin, G. Luo, I. Benjamin and M. L. Schlossman, *J. Chem. Phys.*, 2010, **132**.
20 Z. Samec, V. Marecek, K. Holub, S. Racinsky and P. Hajkova, *J. Electroanal. Chem.*, 1987, **225**, 65–78.
21 Y. I. Kharkats and J. Ulstrup, *J. Electroanal. Chem.*, 1991, **308**, 17–26.
22 B. A. Bauer, Y. Zhong, D. J. Meninger, J. E. Davis and S. Patel, *J. Mol. Graphics Modell.*, 2011, **29**, 876–887.
23 K. Shiratori and A. Morita, *J. Chem. Phys.*, 2011, **134**.
24 H. A. Stern and S. E. Feller, *J. Chem. Phys.*, 2003, **118**, 3401–3412.
25 P. M. Wang and A. Anderko, *Fluid Phase Equilib.*, 2001, **186**, 103–122.
26 L. I. Daikhin, A. A. Kornyshev and M. Urbakh, *J. Electroanal. Chem.*, 2001, **500**, 461–470.
27 L. I. Daikhin and M. Urbakh, *J. Electroanal. Chem.*, 2003, **560**, 59–67.
28 C. Yang and D. Q. Li, *Colloids Surf., A*, 1996, **113**, 51–59.
29 D. Henderson, M. Holovko and A. Trokhymchuk, *Ionic soft matter: modern trends in theory and applications*, Springer, Dordrecht, London, 2005.

